Iranian Journal of Basic Medical Sciences

ijbms.mums.ac.ir

IJBMS

Effect of coating thickness of iron oxide nanoparticles on their relaxivity in the MRI

Farzaneh Hajesmaeelzadeh [1, 2], Saeed Shanehsazzadeh [3], Cordula Grüttner [4], Fariba Johari Daha [3], Mohammad Ali Oghabian [1, 2*]

[1] Biomolecular Imaging Analysis Group, Research Center for Molecular and Cellular Imaging, Tehran University of Medical Sciences, Tehran, Iran
[2] Department of Medical Physics and Biomedical Engineering, Faculty of Medicine, Tehran University of Medical Science, Tehran, Iran
[3] Radiation Application Research School, Nuclear Science and Technology Research Institute, Tehran, Iran
[4] Micromod Partikeltechnologie GmbH, Friedrich-Barnewitz-Str. 4, D-18119 Rostock, Germany

ARTICLE INFO

Article type:
Original article

Article history:
Received: Apr 25,2015
Accepted: Oct 8, 2015

Keywords:
Coating thickness
Hydrodynamic size
Nanoparticles
Relaxivity

ABSTRACT

Objective(s): Iron oxide nanoparticles have found prevalent applications in various fields including drug delivery, cell separation and as contrast agents. Super paramagnetic iron oxide (SPIO) nanoparticles allow researchers and clinicians to enhance the tissue contrast of an area of interest by increasing the relaxation rate of water. In this study, we evaluate the dependency of hydrodynamic size of iron oxide nanoparticles coated with Polyethylene glycol (PEG) on their relativities with 3 Tesla clinical MRI.

Materials and Methods: We used three groups of nanoparticles with nominal sizes 20, 50 and 100 nm with a core size of 8.86 nm, 8.69 nm and 10.4 nm that they were covered with PEG 300 and 600 Da. A clinical magnetic resonance scanner determines the T_1 and T_2 relaxation times for various concentrations of PEG-coated nanoparticles.

Results: The size measurement by photon correlation spectroscopy showed the hydrodynamic sizes of MNPs with nominal 20, 50 and 100 nm with 70, 82 and 116 nm for particles with PEG 600 coating and 74, 93 and 100 nm for particles with PEG 300 coating, respectively. We foud that the relaxivity decreased with increasing overall particle size (via coating thickness). Magnetic resonance imaging showed that by increasing the size of the nanoparticles, r_2/r_1 increases linearly.

Conclusion: According to the data obtained from this study it can be concluded that increments in coating thickness have more influence on relaxivities compared to the changes in core size of magnetic nanoparticles.

► *Please cite this article as:*
Hajesmaeelzadeh F, Shanehsazzadeh S, Grüttner C, Johari Daha F, Oghabian MA. Effect of coating thickness of iron oxide nanoparticles on their relaxivity in the MRI. Iran J Basic Med Sci 2016; 19:166-171.

Introduction

Superparamagnetic iron oxide nanoparticles are of special interest for various applications in biotechnology and biomedicine. One of the most important and rapidly growing fields is the use of iron oxide nanoparticles as negative contrast agents for magnetic resonance imaging (MRI) (1-3). Magnetic nanoparticles (MNPs) are composed of an iron oxide core consisting of crystal magnetite or maghemite. Nowadays, these MNPs are used in different types of studies such as cell tracking, lymph node detection, drug deliveries, and hyperthermia (4-8). In the areas containing the MNPs contrast increases due to disturbance of the MRI signal by the magnetic properties of the iron oxide core (9). Polyethylene glycol (PEG) is a hydrophilic polymer that is stable, biocompatible, and used in drug delivery applications (10). PEG coatings have reduced interactions with the mononuclear phagocyte system and the complement system, and increased nanoparticle circulation time and subsequent accumulation in targeted tissue (11-14).

The ability of a contrast agent to enhance the proton relaxation rate is defined in terms of its relaxivity. The relaxivities of nuclear spins in the aqueous suspension of MNPs can be expressed as:

$$\frac{1}{T_{im}} = \frac{1}{T_i} + r_i . C \qquad \text{Equation (1)}$$

Where i=1 or 2, and $1/T_{im}$ represents the relaxivity of nuclear spins with no nanoparticle contrast agent. r_i is the relaxivity of nuclear spins per ppm of nanoparticles, and C represents the concentration of MNPs in the aqueous suspension.

Relaxivity determines the ability of a fixed **concentra-**tion of the agent to increase relaxation rates, which

*Corresponding author: Mohammad Ali Oghabian. Biomolecular Imaging Analysis Group, Research Center for Molecular and Cellular Imaging, Tehran University of Medical Sciences, Tehran, Iran, Department of Medical Physics and Biomedical Engineering, Faculty of Medicine Tehran University of Medical Science, Tehran, Iran. Tel : +98-21-66907518; Fax: +98-21-664386310; email: oghabian@sina.tums.ac.ir

corresponds to a decrease in relaxation times. Relaxivity is expressed in units of ml, mg $^{-1}$, sec $^{-1}$ of nanoparticles.

The values of the r_1 and r_2 relaxivities increase linearly with increasing particle core size (15). This is because larger iron oxide nanoparticles possess higher magnetization values and exhibit stronger MR contrast effects (16). Although there are several studies, which evaluate the relationship between hydrodynamic size of the MNPs and their relaxivities, there is still a lack of knowledge about effects of hydrodynamic size of PEGylated MNPs on their relaxivities (17-20).

In this study, we evaluate the dependency of hydrodynamic size of PEG coated iron oxide nanoparticles on their relativities in the water phantom with 3 Tesla clinical MRI.

Materials and Methods

Nanomag®-CLD-spio MNPs with PEG, MW=600 Da (PEG 600) and nanomag®-D-spio MNPs with PEG, MW=300 Da (PEG 300) in different hydrodynamic sizes of 20, 50 and 100 nm were used for contrast-enhanced MRI. These nanoparticles were obtained from Micromod Partikeltechnologie GmbH (Germany). The characteristics of the NPs were represented in Table 1.

The particle core size and structure of the PEG-coated nanoparticles were checked with transmission electron microscopy (TEM), PHILIPS, CM 30 (21). Photon correlation spectroscopy (PCS) was used to determine the hydrodynamic particle diameter of the particle samples. The PCS measurements were performed with a Malvern Zeta sizer Nano ZS-90 (Malvern Instruments Ltd., Worcestershire, UK). Iron concentration of suspensions was acquired with inductively coupled plasma atomic emission spectroscopy (ICP-AES, Varian-Liberty, 150 AX Turbo, USA) of digested samples with boiling HNO_3 (5, 6). For the relaxivity measurements, aqueous suspensions of various nanoparticle concentrations were prepared in a water phantom. The T_1 and T_2 relaxation times of hydrogen protons in the aqueous suspension of the coated nanoparticles were measured using an MR scanner (3T Scanner, Siemens, Magnetom Trio).

Relaxivity measurement

Relaxivity is a measure of the ability of a MRI contrast agent to increase the relaxation of the surrounding nuclear spins (hydrogen protons), which can then be used to improve contrast in MR images. We used two groups of MNP samples with nominal sizes of 20, 50 and 100 nm, with varying MNP concentrations of 0.02, 0.01, 0.005, 0.0025, 0.00125 and 0.000625 mg/ml. The first group of MNPs was coated with PEG 600 and the second group was coated with PEG 300. MRI of samples (in test tubes) with various iron concentrations was performed using a 3T MR scanner and a standard circularly polarized head coil (Clinical MR Solutions, Brookfield, WI, USA). All MNPs were placed in a water-containing plastic container at room temperature to avoid susceptibility artifacts from the surrounding air in the scans. T_1 images were attained using six spin echo (SE) images with a fixed echo time (TE=12 msec) and repetition time (TR) values of 200, 400, 1000, 2000, 3000 and 4000 msec. For the T_1 calculation we used a non-linear least-square curve fitting on a pixel-by-pixel basis using MATLAB software (22). Signal intensity as expressed in equation 2:

$$SI_{(\text{pixel xy})} = S_{0_{(\text{pixel xy})}}[1 - e^{\text{TR}/\text{T1}}] \quad \text{Equation (2)}$$

For T_2 maps, four SE images with a fixed TR of 3000 msec, and TE values of 24, 36, 48 and 60 msec were taken (23-25). The signal intensity for each pixel as a function of time is expressed in equation 3:

$$SI_{(\text{pixel xy})} = S_{0_{(\text{pixel xy})}}[e^{\text{TE}/T2}] \quad \text{Equation (3)}$$

Special care was taken to analyze only data points with signal intensities significantly above the noise level. Spin-spin or transverse relaxation time (T_2)-weighted spin echo (SE) images were acquired using variable repetition time (TR) and echo (TE) times of TR/TE= 256 msec/16msec, and TR/TE= 3000 msec/64 msec, and then analyzed qualitatively. All sequences were acquired with a field of view of 160 × 160 mm, a matrix of 256×196 pixels, and slice thickness of 3 mm. Initially, the signal intensities of all test tubes with contrast medium at different iron concentrations were assessed visually (5, 26). For quantitative data analysis, the images were transferred to a local workstation, and the T_1 and T_2 maps were calculated assuming mono-exponential signal decay (2, 27).

Table 1. Core size and hydrodynamic size of nanoparticles

Product name	Surface	Nominal particle diameter [nm]	Measured hydrodynamic diameter [nm]	Iron oxide crystal size [nm]
nanomag®-CLD[1]-spio	PEG 300	20	74, PdI: 0.161	8.86±1.61
nanomag®-CLD-spio	PEG 300	50	93, PdI: 0.172	8.69±1.73
nanomag®-CLD-spio	PEG 300	100	100, PdI: 0.311	10.4±1.98
nanomag®-D[2]-spio	PEG 600	20	70, PdI: 0.172	8.86±1.61
nanomag®-D-spio	PEG 600	50	82, PdI: 0.166	8.69±1.73
nanomag®-D-spio	PEG 600	100	116, PdI: 0.152	10.4±1.98

[1] Cross-linked dextran iron oxide composite particle suspension in water
[2] Dextran iron oxide composite particle suspension in water

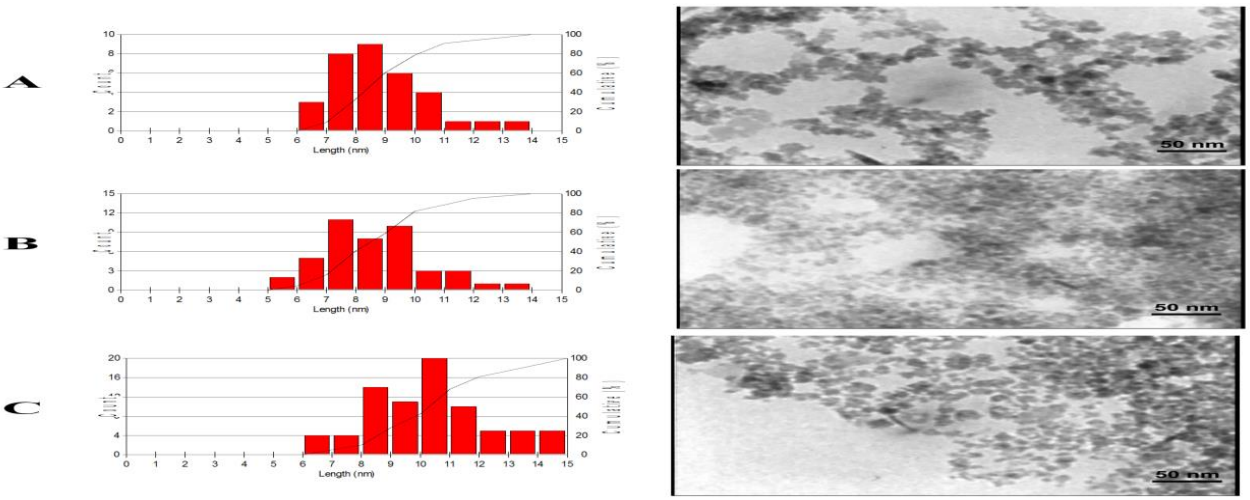

Figure 1. TEM image and histogram of PEGylated iron oxide nanoparticles. A. 20 nm, B. 50 nm and C. 100 nm.

Results

Figure 1 shows TEM images of the PEGylated magnetic nanoparticles. The nominal 20, 50 and 100 nm PEG coated nanoparticles are spherical, with average iron oxide crystal diameters of 8.86 nm, 8.69 nm, and 10.4 nm, respectively.

The size measurement by photon correlation spectroscopy (PCS) showed the hydrodynamic sizes of MNPs of 70, 82 and 116 nm for particles with PEG 600 coating and 74, 93 and 100 nm for particles with PEG 300 coating, respectively (Figure2).

The trends of 1/T2 and 1/T1 of MNPs in presence of different iron concentrations were represented in Figure 2.

Table 2. r_1 and r_2 value of iron oxide nanoparticles

Samples	r_2 [mmol^{-1}sec^{-1}]	r_1[mmol^{-1}sec^{-1}]
PEG 600, 100 nm	18.33	0.58
PEG 600, 50 nm	27.76	0.67
PEG 600, 20 nm	31.44	0.91
PEG 300, 100 nm	10.69	0.16
PEG 300, 50 nm	11.33	0.19
PEG 300, 20 nm	13.12	0.22

The longitudinal and transverse relaxivities were obtained by calculating the slope of the above graphs. The results of these calculations are presented in Table 2. r_1 and r_2 relaxivity decreased by increasing particle size, in both groups (Figure 3).

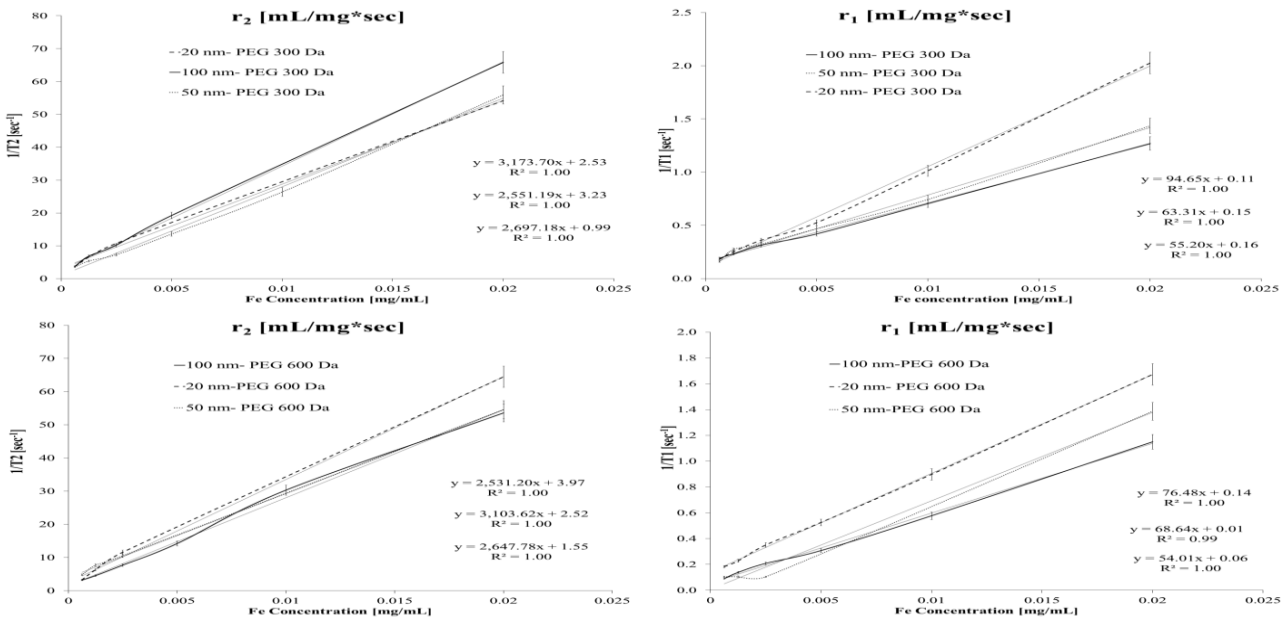

Figure 2. Plot of $1/T_2$ and $1/T_1$ versus Fe concentration. The slope of the line represents the longitudinal and transverse relaxivity

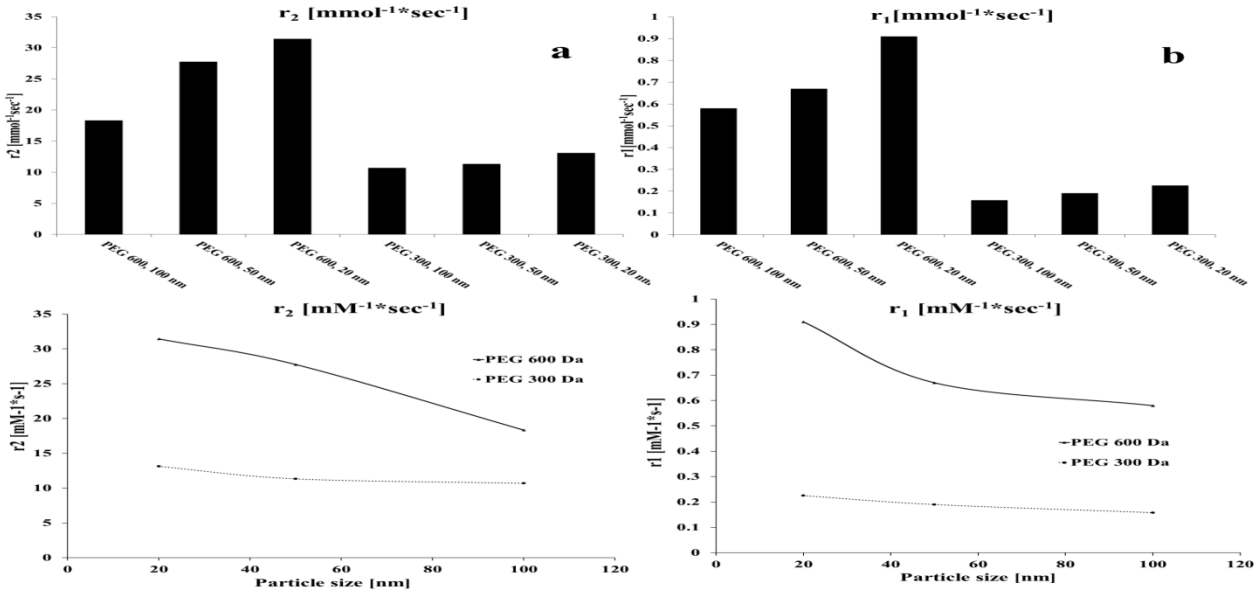

Figure 3. Plots of (a) r_2 and (b) r_1 relaxivity versus particle size of PEGylated iron oxide nanoparticles

Discussion

TEM studies showed a similar core size of 8–10±2 nm independent of the chemical coating (Figure 1) and PCS showed that the hydrodynamic sizes of the particles increased with increasing coating thickness (Table 1). Figure 2 and Figure 3 clearly demonstrate the trends in r_1 and r_2 changes after increasing the hydrodynamic size by coating thickness.

LaConte *et al* tried to evaluate the effect of coating thickness on the relaxivity of PEGylated mono crystalline super paramagnetic iron oxide nanoparticles (MIONs) (17). In their study, the r_1 and r_2 of MIONs were measured using a bench-top nuclear magnetic resonance (NMR) relaxometer. They also estimated the proton movement in a field with nanometer-sized magnetic particles in homogeneities via Monte Carlo simulations. They concluded that coating thickness could significantly influence the r_2 and the r_2/r_1 ratio of a MION contrast agent. For example, their simulations showed that while coating thickness increased, the r_2 decreased and the r_1 increased (17). However, as represented in our experimental data in Figure 2 and Figure 3 both r_1, r_2 and even r_1 and r_2 decreased when coating thickness increased.

Ahmad *et al.* investigated the particle size dependence of the relaxivity of hydrogen protons in an aqueous suspension of silica coated iron oxide (Fe_3O_4) nanoparticles. They concluded that the relaxivity increased linearly with increasing particle size (15). In their study, they showed that by increasing the core size of MNPs with the magnitude of 17% the r_1 and r_2 increased with the magnitude of 13% and 22%, respectively (15). On the other hand, in our study of the 20 nm and 50 nm NPs with a PEG 300 coating the MNPs have the same iron oxide core size (8.78 nm) and a different coating thickness (74 nm, 93 nm), but our results indicate that an increase in 26% in the coating thickness resulted in a decrease of r_1 and r_2 by the cofactor 13.64%. In addition, for the 20 and 50 nm NPs coated with PEG 600 with the same core size (8.78 nm) and different coating thickness of 70 and 82 nm our results show that an increasing coating thickness by 17% led to a decrease of r_1 and r_2 by factors of 26% and 12%, respectively. These results clearly indicate that a decrease of r_1 and r_2 is due to the increments in coating thickness.

In terms of 20 and 100 nm NPs coated with PEG 300, our size measurement revealed about 18.5% core size increments and 35% increments in coating thickness. However, the relaxivity studies showed that the r_1 and r_2 values decreased by 27.27% and 18.52%, respectively. These findings were in contrast to the results of Ahmad *et al.*, which expect more than 17% and 25% increments in r_1 and r_2 values, respectively. This discrepancy is mainly due to coating thickness increments, which was not considered in previous studies. Our results indicate that changes in hydrodynamic size (coating thickness) influence the relaxivity more than core size alterations. The comparison of the relaxivity changes between 50 and 100 nm NPs coated with PEG 300 demonstrated that while the core size was increased by 18.5% and the coating thickness by 8% again both r_1 and r_2 decreased by the magnitude of 15.79% and 5.65%, respectively. These data seem logical because the hydrodynamic size increments were less than in our previous studies

about nanoparticles with diameters of 20 and 100 nm. Thus, for the particles used in our study, the decrease of r_1 and r_2 with increasing overall particle size (via coating thickness) can be attributed to the effect of hydrodynamic particle size.

This study is the continuation of our previous study on the effect of functional group and surface charge of MNPs on their relaxivity constant (28). In that study, we concluded that particles with positive surface charges showed higher r_2/r_1 ratios (28). We examined the r_1 for particles with same charge (negative charge) and functional group (COOH) with two different hydrodynamic sizes of 59.4 and 67.4 and r_1 values of 0.17 and 0.31 (mM^{-1} sec^{-1}), respectively. This discrepancy in T_1 (r_1) can be justified with the fact that dependency of T_1 on molecular rotation movements can be affected by hydrodynamic size. This is in accordance with the findings represented in Figure 3 (28). In summary, this study indicates an ignored factor in relaxivity and can be a trigger for more theoretical and experimental work on the effect of coating thickness on relaxivity.

Conclusion

In this study, we examined the effect of hydrodynamic size of the iron oxide nanoparticles coated with PEG on the relaxivity. In summary, based on the results of this study, the r_1 and r_2 value decrease with increasing hydrodynamic size. Our finding is in contrast to some other studies, which neglect the impact of coating thickness. As a result, by increasing hydrodynamic size (via coating thickness), the longitudinal and transverse relaxivity linearly decrease. This effect may be caused by the physical exclusion of protons from the magnetic field.

Acknowledgment

The authors should thank to Micromod Company for their supports in terms of nanoparticles providing and the quantitative analysis of the particles. The results described in this paper were part of student thesis. Council of Research of Tehran University of Medical Sciences (TUMS), Tehran, Iran, supported this work.

Conflict of interest

The authors declare that they have no conflict of interest.

References

1. Gamarra L, Pontuschka WM, Amaro E, Costa-Filho A, Brito G, Vieira E, et al. Kinetics of elimination and distribution in blood and liver of biocompatible ferrofluids based on Fe 3 O 4 nanoparticles: An EPR and XRF study. Mater Sci Eng C 2008;28:519-25.
2. Shanehsazzadeh S, Gruettner C, Lahooti A, Mahmoudi M, Allen BJ, Ghavami M, *et al*. Monoclonal antibody conjugated magnetic nanoparticles could target MUC-1-positive cells in vitro but not *in vivo*. Contrast Media Mol Imaging 2015; 10:225–36.
3. Zhao X, Zhao H, Chen Z, Lan M. Ultrasmall superparamagnetic iron oxide nanoparticles for magnetic resonance imaging contrast agent. J Nanosci Nanotechnol 2014; 14:210-20.
4. Shanehsazzadeh S, Oghabian MA, Allen BJ, Amanlou M, Masoudi A, Daha FJ. Evaluating the effect of ultrasmall superparamagnetic iron oxide nanoparticles for a long-term magnetic cell labeling. J Med Phys 2013; 38:34.
5. Shanehsazzadeh S, Oghabian MA, Lahooti A, Abdollahi M, Haeri SA, Amanlou M, et al. Estimated background doses of [67Ga]-DTPA-USPIO in normal Balb/c mice as a potential therapeutic agent for liver and spleen cancers. Nucl Med Commun 2013; 34:915-25.
6. Mahmoudi M, Sant S, Wang B, Laurent S, Sen T. Superparamagnetic iron oxide nanoparticles (SPIONs): development, surface modification and applications in chemotherapy. Adv Drug Deliv Rev 2011; 63:24-46.
7. Bagheri-abassi F, Alavi H, Mohammadipour A, Motejaded F. Ebrahimzadeh-bideskan, A., The effect of silver nanoparticles on apoptosis and dark neuron production in rat hippocampus. Iran J Basic Med Sci 2015,18, 644-648.
8. Mayelifar K, Taheri AR, Rajabi O, Sazgarnia A. Ultraviolet B efficacy in improving antileishmanial effects of silver nanoparticles. Iran J Basic Med Sci 2015, 18, 677-683.
9. Lind K, Kresse M, Debus NP, Müller RH. A novel formulation for superparamagnetic iron oxide (SPIO) particles enhancing MR lymphography: comparison of physicochemical properties and the *in vivo* behaviour. J Drug Target 2002;10:221-30.
10. Mahmoudi M, Simchi A, Imani M, Hafeli UO. Superparamagnetic iron oxide nanoparticles with rigid cross-linked polyethylene glycol fumarate coating for application in imaging and drug delivery. J Phys Chem C 2009; 113:8124-31.
11. Harris JM, Chess RB. Effect of pegylation on pharmaceuticals. Nat Rev Drug Discov 2003; 2:214-21.
12. Moghimi SM, Hunter AC, Murray JC. Long-circulating and target-specific nanoparticles: theory to practice. Pharmacol Rev 2001;53:283-318.
13. Carroll MC. The complement system in regulation of adaptive immunity. Nat Immunol 2004;5:981-6.
14. Ni F, Jiang L, Yang R, Chen Z, Qi X, Wang J. Effects of PEG length and iron oxide nanoparticles size on reduced protein adsorption and non-specific uptake by macrophage cells. J Nanosci Nanotechnol 2012;12:2094-100.
15. Ahmad T, Bae H, Rhee I, Chang Y, Lee J, Hong S. Particle size dependence of relaxivity for silica-coated iron oxide nanoparticles. Curr Appl Phys 2012;12:969-74.
16. Wang C, Chen J, Talavage T, Irudayaraj J. Gold Nanorod/Fe3O4 Nanoparticle "Nano-Pearl-Necklaces" for Simultaneous Targeting, Dual-Mode

Imaging, and Photothermal Ablation of Cancer Cells. Angew Chem 2009;121:2797-801.
17. LaConte LE, Nitin N, Zurkiya O, Caruntu D, O'Connor CJ, Hu X, *et al*. Coating thickness of magnetic iron oxide nanoparticles affects R2 relaxivity. J Magn Reson Imaging 2007;26:1634-41.
18. Tromsdorf UI, Bigall NC, Kaul MG, Bruns OT, Nikolic MS, Mollwitz B, et al. Size and surface effects on the MRI relaxivity of manganese ferrite nanoparticle contrast agents. Nano Lett 2007;7:2422-7.
19. Duan H, Kuang M, Wang X, Wang YA, Mao H, Nie S. Reexamining the effects of particle size and surface chemistry on the magnetic properties of iron oxide nanocrystals: new insights into spin disorder and proton relaxivity. J Phys Chem C 2008;112:8127-31.
20. Thanh NT. Magnetic nanoparticles: from fabrication to clinical applications: CRC press; 2012.
21. Khameneh B, Halimi V, Jaafari MR, Golmohammadzadeh S. Safranal-loaded solid lipid nanoparticles: evaluation of sunscreen and moisturizing potential for topical applications. Iran J Basic Med Sci 2015;18:58-63.
22. Lahooti A, Shanehsazzadeh S, Oghabian M A, Allen BJ. In Assessment of human effective absorbed dose of Tc-99m-USPIO based on biodistribution rat data. J Label Compd Rad 2013; S258-S258.
23. Jahanbakhsh R, Atyabi F, Shanehsazzadeh S, Sobhani Z, Adeli M, Dinarvand R. Modified Gadonanotubes as a promising novel MRI contrasting agent. Daru 2013;21:53-61.
24. Omid H, Oghabian MA, Ahmadi R, Shahbazi N, Hosseini HRM, Shanehsazzadeh S, *et al*. Synthesizing and staining manganese oxide nanoparticles for cytotoxicity and cellular uptake investigation. BBA-Gen Subjects 2014;1840:428-33.
25. Müller-Bierl B, Louis O, Fierens Y, Buls N, Luypaert R, de Mey J. Cylinders or walls? A new computational model to estimate the MR transverse relaxation rate dependence on trabecular bone architecture. Magn Reson Mater Phys Biol Med 2014;27:349-61.
26. Galassi F, Brujic D, Rea M, Lambert N, Desouza N, Ristic M. Fast and accurate localization of multiple RF markers for tracking in MRI-guided interventions. Magn Reson Mater Phys Biol Med 2015;28:33-48.
27. Marshall I, Jansen MA, Tao Y, Merrifield GD, Gray GA. Application of kt-BLAST acceleration to reduce cardiac MR imaging time in healthy and infarcted mice. Magn Reson Mater Phys Biol Med 2014;27:201-10.
28. Wang Y-XJ, Hussain SM, Krestin GP. Superparamagnetic iron oxide contrast agents: physicochemical characteristics and applications in MR imaging. Eur Radiol 2001;11:2319-31.